Published in:

Analytical and Bioanalytical Chemistry (2015), 407:1357-69

The final publication is available at Springer via https://doi.org/10.1007/s00216-014-8307-5

Biosynthesis of Seven Carbon Thirteen Labeled *Alternaria* Toxins including Altertoxins, Alternariol, and Alternariol Methyl Ether, and their Application to a Multiple Stable Isotope Dilution Assay

Yang Liu[a] and Michael Rychlik[a,b] *

[a] Chair of Analytical Food Chemistry, Technische Universität München, Alte Akademie 10, D-85354 Freising, Germany

[b] BIOANALYTIK Weihenstephan, ZIEL Research Center for Nutrition and Food Sciences, Technische Universität München, Alte Akademie 10, D-85354 Freising, Germany

STABLE ISOTOPE DILUTION ASSAY of *Alternaria* Toxins

* Corresponding Author.

Phone: + 49 8161 71 3153.

Fax: + 49 8161 71 4216.

E-Mail: michael.rychlik@tum.de.

Abstract

An unprecedented stable isotope dilution assay for the genotoxic altertoxins along with exposure data of consumers is presented to enable a first risk assessment of these *Alternaria* toxins in foods.

Altertoxins were produced as the most abundant *Alternaria* toxins in a modified Czapek–Dox medium with a low level of glucose as the carbon source and ammonium sulphate as the sole nitrogen source.

Labeled altertoxins were synthesized in the same way using [$^{13}C_6$]glucose. Moreover, labeled alternariol, alternariol methyl ether, altenuene, and alternuisol were biosynthesized in another modified medium containing [$^{13}C_6$]glucose and sodium [$^{13}C_2$]acetate. A stable isotope dilution LC–MS/MS method was developed and used for food analysis. For altertoxin I, altertoxin II, alterperylenol, alternariol, and alternariol methyl ether, the limits of detection ranged from 0.09 to 0.53 μg kg^{-1}. The inter- /intra-day (n=3×6) relative standard deviations of the method were below 13%, and the recoveries ranged between 96 and 109%. Among the various commercial food samples, some of the organic whole grains revealed low-level contamination with altertoxin I and alterperylenol, and paprika powder, which was heavily loaded with alternariol, alternariol methyl ether, and tentoxin, showed higher contamination level of altertoxin I and alterperylenol. Altertoxin II and III and stemphyltoxin III were not detectable. In addition, if the food was contaminated with altertoxins, it was likely to be co-contaminated with the other *Alternaria* toxins, but not necessarily vice versa. Maximum concentrations of altertoxin I and alterperylenol were 43 and 58 μg kg^{-1} detected in sorghum feed samples. This was significantly higher than that in the measured food samples.

Keywords altertoxin; alternariol; alternariol methyl ether; *Alternaria*; mycotoxin; stable isotope dilution assay

Introduction

Altertoxin (ATX) I, II, III, alterperylenol, and stemphyltoxin III (Ste III) are perylenquinone derivatives produced by *Alternaria* spp., such as *Alternaria alternata* [1], *Alternaria mali* [2], *Alternaria eichorniae* [3], and *Stemphylium* sp. [4]

<<**Fig. 1** Structures of ATXs>>

Pero et al. first isolated ATX I and II in 1973 and indicated considerable cytotoxicity of these *Alternaria* metabolites. In particular ATX II was reported to be highly toxic against the cervical cancer cell line HeLa, with the median inhibitory dose of cell growth (IhD_{50}) of 0.5 μg mL^{-1}, compared with the IhD_{50} values for the other *Alternaria* toxins alternariol (AOH), ATX I, and tenuazonic acid of 6 μg mL^{-1}, 20 μg mL^{-1} and above 40 μg mL^{-1}, respectively [2]. In 1983, Okuno et al. elucidated the correct structures of ATX I and alterperylenol and proposed a possible biosynthetic route involving a polyketide pathway [5]. Regarding mutagenicity, ATX III, II and I have been reported to show a mutagenic potency of approximately 0.7, 0.5, and less than 0.03 revertants per pmol with *S. typhimurium* TA100 [6]. Recently it has been reported that ATX II is at least 50-times more potent as a mutagen than the common *Alternaria* toxins AOH and alternariol methyl ether (AME) in cultured Chinese hamster V79 cells [7].

Considering the mutagenic and possibly carcinogenic potency of ATXs, an efficient analytical method should be established for a substantial risk evaluation [8]. In particular, the lack of substantial exposure data was the reason that ATXs were excluded from a recent Scientific

Opinion on the risks of Alternaria toxins presented by the European Food Safety Authority (EFSA) Panel on Contaminants in the Food Chain [9].

Analytical methods including HPLC–UV and TLC methods have been developed to determine ATX I in juices, and the matrix-dependent limits of detection (LODs) ranged from 70 to1000 μg kg^{-1} [10]. Moreover, a HPLC method with electrochemical detection was developed to monitor ATX I and ATX II at sub-ppm levels from extracts of artificially infected maize [11]. Heavy ATX I contamination was found in infected wheat and sorghum [12,13].

Recently, ATX I has been included in some multi-mycotoxin LC–MS/MS methods using external calibration [14-17]. The lowest demonstrated LOD was 3 μg kg^{-1} [14]. However, for commercial food analysis, the sensitivity and selectivity of previously established methods are inadequate.

Therefore, the purpose of this study was to develop a validated isotope dilution LC–MS/MS method for ATX I, II, and alterperylenol. Additionally, the dibenzopyrone derivatives AOH and AME and the phytotoxic cyclic peptide tentoxin (TEN), which have been frequently detected in food were included in this multiple method to observe distributions of these toxins in food.

<<**Fig. 2** Structures of AOH, AME, and TEN>>

Materials and methods

Chemicals and reagents

Ammonium sulphate, citric acid, copper (II) sulphate pentahydrate, glucose, iron (II) sulphate heptahydrate, and potassium chloride were purchased from Merck (Darmstadt, Germany). Manganese (II) sulphate monohydrate, potassium dihydrogen phosphate, sodium molybdate

dihydrate, sodium nitrate, zinc sulphate monohydrate, maltose, and reference materials of AOH and AME were obtained from Sigma-Aldrich (Steinheim, Germany). Boric acid was purchased from Avantor Performance Materials (Deventer, The Netherlands), and magnesium sulphate heptahydrate was purchased from AppliChem (Darmstadt, Germany). [$^{13}C_6$]Glucose (>99 atom% ^{13}C) and [$^{13}C_2$]sodium acetate (>99 atom% ^{13}C) were obtained from Euriso-top (Saarbrücken, Germany). D_4-MeOH (>99 atom% D) was from Euriso-top (Gif sur Yvette Cedex, France). ACS grade dichloromethane (DCM) was obtained from Merck (Darmstadt, Germany). LC–MS grade acetonitrile (ACN), 2-propanol, and methanol (MeOH) were purchased from VWR Prolabo (Fontenay Sous Bois, France). [$^{2}H_4$]AOH, [$^{2}H_4$]AME, and [$^{2}H_3$]TEN were synthesized as reported earlier [19,20].

Instrumentation

Products were purified by a LaChrom HPLC system (Merck/Hitachi, Tokyo, Japan) using a YMC-Pack Pro C-18 preparative column (150×20 mm, 10 µm, 120 Å, YMC, Dinslaken, Germany) applying the gradient elution detailed in table S-2 in the Electronic Supplementary Material. LC–MS/MS was performed on a Shimadzu LC-20A Prominence system (Shimadzu, Kyoto, Japan) using a Hyperclone BDS C-18 column (150×3.2 mm, 3 µm, 130 Å, Phenomenex, Aschaffenburg, Germany) interfaced to a hybrid triple quadrupole/linear ion trap mass spectrometer (4000 QTrap, Applied Biosystems, Foster City, CA, USA). The UV absorption was recorded on an UV spectrometer Specord 50 (Analytik Jena, Jena, Germany). The purified compounds were characterized by ^{1}H-NMR on a Bruker AV III system (Bruker, Rheinstetten, Germany) operating at 500 MHz. All compounds were dissolved in D_4-MeOH.

Biosyntheses

Synthesis of ATX standards in rice culture:

To 25 g parboiled rice, 15 mL distilled water was added in a 250 mL polycarbonate Erlenmeyer flask, and the flask was sterilized at 121°C for 20 min. It was then inoculated with a loop of *Alternaria alternata* conidia (obtained from the Chair of Phytopathology, TU München), which was isolated from a potato leaf of a field trial in Freising at the end of the potato early blight epidemics in 2012. The culture was left at room temperature for 37 days. Subsequently, the mouldy rice was finely homogenized using a mortar and pestle and extracted with DCM (2×100 mL) on a shaker at 110 rpm for 6 h. The extract was evaporated under vacuum and the brown-red residue was dissolved in 3 mL of ACN–H_2O (50:50, v/v), filtered, and purified by preparative HPLC detailed above. Purity was assessed by integration of the HPLC peak areas at 254 nm eluted isocratically with different mixtures of ACN and water. ATX I (244 µg, >99% pure), alterperylenol (60 µg, >99% pure), ATX II (177 µg, >97% pure), and Ste III (171 µg, >98% pure) were collected. Analytical data of the products are shown in **Table 1**. All ^{1}H-NMR data are in agreement with the literature [21,22]. Maximum wavelengths of the UV absorption are in good agreement with the literature as well, whereas the absorption coefficients deviate from the highly inconsistent literature data [1,21,23].

<< **Table 1.** Characterization of ATXs >>

Synthesis of [$^{13}C_{20}$]ATXs in synthetic medium:

Twenty-five mL of modified Czapek–Dox medium was prepared in a 250 mL polycarbonate Erlenmeyer flasks, containing [$^{13}C_6$]glucose (4 g L^{-1}), KCl (0.5 g L^{-1}), KH_2PO_4 (1 g L^{-1}),

$MgSO_4 \cdot 7H_2O$ (0.5 g L^{-1}), $(NH_4)_2SO_4$ (0.27 g L^{-1}), $FeSO_4 \cdot 7H_2O$ (0.01 g L^{-1}), and a solution of trace elements (100 mL aqueous solution containing citric acid 5 g, $ZnSO_4 \cdot 6H_2O$ 5 g, $Fe_2(NH_4)_2(SO_4)_2 \cdot 6H_2O$ 1 g, $CuSO_4 \cdot 5H_2O$ 250 mg, $MnSO_4$ 50 mg, H_3BO_3 50 mg, and $Na_2MoO_4 \cdot 6H_2O$ 50 mg) (2 mL L^{-1}) [24]. The pH was adjusted to 5.5. The medium was sterilized at 121°C for 20 min. The cooled medium was inoculated with the *Alternaria alternata* strain that was also used to prepare the unlabeled toxins. The culture was then incubated on a shaker at 110 rpm at 26°C for 7 days in darkness. After 7 days the culture broth was filtered. The aqueous solution was extracted with ethyl acetate (2×20 mL). The residue was homogenized using the mortar and pestle, and extracted with DCM–MeOH (1:1, v/v; 2×25 mL) on a shaker at 110 rpm for 3 h. The combined extracts were evaporated under vacuum and the brown-red residue was dissolved in 1 mL of ACN–H_2O (50:50, v/v) and purified by preparative HPLC.

Synthesis of [$^{13}C_{14}$]AOH and [$^{13}C_{15}$]AME in synthetic medium:

Twenty-five mL of modified Czapek–Dox medium was prepared in a 250 mL polycarbonate Erlenmeyer flask, containing [$^{13}C_6$]glucose (8 g L^{-1}), KCl (0.5 g L^{-1}), KH_2PO_4 (1 g L^{-1}), $MgSO_4 \cdot 7H_2O$ (0.5 g L^{-1}), $(NH_4)_2SO_4$ (0.27 g L^{-1}), $FeSO_4 \cdot 7H_2O$ (0.01 g L^{-1}), and [$^{13}C_2$]NaOAc (0.8 g L^{-1}). The pH was adjusted to 5.5. Incubation with the same *Alternaria alternata* strain and extraction of the medium were performed analogously to the procedure described above for altertoxins. After several preparative HPLC runs, 5 µg of [$^{13}C_{14}$]AOH and [$^{13}C_{15}$]AME were collected, quantified by UV spectrometer using the verified absorption coefficient [19], and prepared in ACN as internal standards for food analysis.

150 [$^{13}C_{15}$]altenuene (ALT) and [$^{13}C_{14}$]altenuisol (AS) were also collected from this system and were
151 used for qualitative detection of the unlabeled analytes. Mass spectral properties of the ^{13}C-
152 labeled toxins are shown in **Table 2**.

153 << **Table 2.** MS fragmentation of ^{13}C-labeled toxins >>

154 **Quantitative NMR**

155 Quantitative NMR measurement was performed analogously to the method described by Korn et
156 al. [25] Briefly, the purified compounds were dissolved in 200 µL of D_4-MeOH in 3×103.5 mm
157 NMR tubes (ST500-7, Norell, Landisville, USA) and directly analysed on the Bruker AV III
158 system. Maltose was used as external calibration standard. The aromatic proton (doublet) of the
159 toxins and the anomeric proton signal of maltose at 5.25 ppm (doublet) were chosen for
160 quantitation. Peaks were integrated manually. Accuracy of the quantitative NMR measurement
161 was within a range of 2 %.

162 **Preparation of standard solutions**

163 Stock solutions of labeled and unlabeled ATXs were prepared in MeOH shortly after the NMR
164 measurement and stored at –20°C. Stability was examined after 6 months by HPLC–UV. AOH
165 and AME standard concentrations were calculated using the measured UV absorption at 256 nm
166 with 1 cm path length and the extinction coefficient of 40600 L mol^{-1} cm^{-1} for AOH and 47600 L
167 mol^{-1} cm^{-1} for AME in ACN [19]. For calibration they were further diluted to 1 µg mL^{-1} and 0.1
168 µg mL^{-1}.

LC–MS/MS measurement

The binary gradient system consisted of (A) ACN–2-propanol–H_2O (17.5: 17.5: 65, v/v/v) and (B) MeOH at a flow rate of 0.2 mL min^{-1}. The gradient started at 0% B for 3 min and was raised linearly from 0% B to 100% B during the next 22 min and maintained at 100% B for 2 min. Thereafter, the mobile phase returned to 0% B within 2 min, and the system was equilibrated for 5 min before the next run. The injection volume was 5 μL.

he ion source parameters were set as follows: curtain gas 10 psi, CAD gas pressure medium, ion spray voltage –4500 eV, spray gas 45 psi, dry gas 55 psi, temperature 450°C. MS parameters were optimized by direct infusion of each standard solution (100 ng mL^{-1}) into the source. For MS/MS measurements, the mass spectrometer was operated in the multiple reaction monitoring (MRM) mode at the conditions detailed in **Table 3**. A Rheodyne valve (IDEX Health & Science, Oak Harbor, WA, USA) was used to divert the column effluent to the mass spectrometer from 7 to 22 min and to waste for the rest of the run. Data acquisition was carried out using Analyst 1.5 software (Applied Biosystems, Foster City, CA, USA).

<< **Table 3**. Compound-dependent parameters for MRM (negative) mode in LC–MS/MS.>>

Calibration and quantitation

A series of solutions with constant amounts of internal standard (IS) and varying amounts of analyte (An) in molar ratios between 0.1 to 10 (1:10, 1:5, 1:2, 1:1, 2:1, 5:1, 10:1) were prepared for the calibration curves of ATX I, II, alterperylenol, AOH, and AME. Peak area (A) ratios [A(An)/A(IS)] were then obtained via LC–MS/MS, and a response curve was calculated from molar ratios [n(An)/n(IS)] versus [A(An)/A(IS)]. Calibration functions were obtained using

simple linear regression and revealed a negligible intercept. Linearity of the response was checked by analysis of the residuals (homogeneity and normal distribution) after linear regression and the Mandel-test for suitability of a linear approximation was performed.

Sampling and sample preparation

Food samples were collected from markets in and around Freising, Germany. For solid samples, 0.5–1 g of the finely ground (particle diameter <500 µm) and homogenized sample was spiked with a mixture (30 µl) of [$^{13}C_{20}$]ATX I (300 ng mL^{-1}), [$^{13}C_{20}$]alterperylenol (180 ng mL^{-1}), [$^{13}C_{20}$]ATX II (90 ng mL^{-1}), [$^{13}C_{14}$]AOH (260 ng mL^{-1}), [$^{13}C_{15}$]AME (90 ng mL^{-1}), and [$^{2}H_{3}$]TEN (40 ng mL^{-1}). Then 10 mL of ACN–H_2O (84:16, v/v) was added to the sample, and the mixture was briefly vortexed and shaken on a laboratory shaker at 200 rpm for 1.5 h. Subsequently, the sample was centrifuged at 1000 *g* for 10 min. The supernatant was defatted with pentane (3×6 mL), diluted with the same volume of water, if necessary clarified by adding saturated sodium chloride solution (approx. 1.5 mL), and extracted with DCM (2×5 mL). The extract was evaporated to dryness, dissolved in 200 µL of MeOH–H_2O (50:50, v/v), and filtered through a 0.22 µm membrane filter (Berrytech, Grünwald, Germany) prior to LC–MS/MS.

For liquid samples, 20 g of sample was spiked with the same amount of internal standards as above for solid samples, diluted with 5 mL of saturated sodium chloride solution, and extracted with DCM (2×5 mL). The extract was evaporated to dryness, dissolved in 200 µL of MeOH–H_2O (50:50, v/v), and filtered through a 0.22 µm membrane filter prior to LC–MS/MS.

Method validation

Method validation was carried out in analogy to the validation procedure described for TEN [20].

Limits of detection and limits of quantitation (LOQs). Potato starch was used as blank matrix and spiked with unlabeled compounds at 0.4, 0.8, 1.6, and 4 μg kg^{-1} (each in triplicate). Analysis was performed as described above. Then the data obtained from the stable isotope dilution assays (SIDAs) and spiked amounts were correlated. A subsequent regression calculation provided the calibration line and the confidence interval, which was used to compute the LODs and LOQs [26].

Precision. Naturally contaminated organic whole wheat flour with ATX I and AOH concentrations at 4.0 and 23 μg kg^{-1}, respectively, and potato starch spiked with alterperylenol, ATX II, and AME (each at 4.0 μg kg^{-1}) were used to determine inter-day (n=3 within 3 weeks) and intra-day (n=6 on each of those 3 days) precision.

Recovery of SIDA. Recovery was calculated from the results of spiked potato starch used for LOD/LOQ determination.

Results and discussion

Biosynthesis

The total amount of ATXs increased during 14 days of cultivation in rice medium and remained at a relatively high level even until 37 days of incubation; longer incubation times were not investigated. By the 37^{th} day of incubation, TEN was degraded completely, AOHs were degraded to a great extent, and ATXs were then purified by preparative HPLC.

In the synthetic medium with higher concentration of glucose (50 g L^{-1}) and sodium nitrate the fungus did not produce significant amounts of ATXs even after months, although more biomass was formed. Since ATXs were observed as the main toxins produced during fungal growth in rice

232 in the later phase, it was assumed that NH_4^+, which is the degradation form of nitrogen
233 originating e.g. from proteins, might be essential for ATX biosynthesis. To prove this, NH_4^+ was
234 used as the sole nitrogen source, and ATXs were produced on a short timescale in liquid medium
235 as the main toxin products in contrast to TEN, AOH, AS, and AME, which were not detected.
236 Obviously NH_4^+ instead of NO_3^- has a direct impact on the ATXs biosynthesis. In summary,
237 modified Czapek–Dox medium containing glucose (4 g L^{-1}) and ammonium sulphate (0.27 g L^{-1})
238 achieved the highest yield, observed in 7–9 days.

239 Subsequently, 25 mL of this optimized medium containing [$^{13}C_6$]glucose was used to produce the
240 labeled internal standards [$^{13}C_{20}$]ATX I (33 µg), [$^{13}C_{20}$]alterperylenol (13 µg), [$^{13}C_{20}$]ATX II (20
241 µg), and [$^{13}C_{20}$]Ste III (20 µg). The yield of [$^{13}C_{20}$]ATX I was approx. 1.1 mg per g dry biomass
242 and 0.33 mg per g glucose, respectively. The isotopologic distribution was similar for all ATXs
243 as recorded in enhanced resolution mode: [$^{13}C_{20}$]isotopologue 100%, [$^{13}C_{19}{}^{12}C_1$]isotopologue
244 39%, [$^{13}C_{18}{}^{12}C_2$]isotopologue 40%, [$^{13}C_{17}{}^{12}C_3$]isotopologue 7%, [$^{13}C_{16}{}^{12}C_4$]isotopologue 11%.

245 **Stability of ATXs**

246 After 6 months of storage in MeOH at –20°C, recoveries of ATX I (10 µg mL^{-1}), alterperylenol
247 (6 µg mL^{-1}), ATX II (5 µg mL^{-1}), and Ste III (25 µg mL^{-1}) determined by HPLC–UV were 97,
248 97, 104, and 93%, respectively, with relative standard deviation (RSD) of less than 10%.
249 However, only 39% were recovered if Ste III was stored at 5 µg mL^{-1} under the same conditions.

Fragmentation in tandem mass spectroscopy

Labeled (m/z value in parentheses) and unlabeled fragments were correlated according to their mass increments and their abundance. Accordingly, a fragmentation scheme is proposed utilizing the number of lost carbons in **Fig. 3**.

<<**Fig. 3** Proposed fragmentation of ATXs. In parentheses the respective *m/z* data of the completely ^{13}C-labeled isotopologue are given.>>

In a previous work of our group, [$^{2}H_4$]AOH and [$^{2}H_4$]AME have been synthesized and characterized [19]. The study presented here provides complementary information via the introduced ^{13}C-labels and, following both spectra, fragmentation pathways are proposed in **Fig. 4–5**.

<<**Fig. 4** MS spectra of labeled and unlabeled AOH and proposed fragmentation to the quantifier. In parentheses: the respective *m/z* data of the completely ^{13}C-labeled isotopologue. In square brackets: the respective *m/z* data of the isotopologue with four ^{2}H-labelings in the aromatic rings.>>

The spectra showed patterns of H-radical loss, e.g. in the *m/z* range of 212–215. Main possible fragments have been discussed before, which are consistent with the ^{13}C-labeled spectrum [19,27]. According to the spectra of the labeled isotopologues, the quantifier fragment (a) at *m/z* 147 of AOH must have lost five carbon atoms and one aromatic hydrogen (**Fig. 4**).

<<**Fig. 5** MS spectra of labeled and unlabeled AME and proposed fragmentation. In parentheses: the respective m/z data of the completely ^{13}C-labeled isotopologue. In square brackets: the respective m/z data of the isotopologue with four ^{2}H-labelings in the aromatic rings.>>

For AME, the fragmentation scheme is proposed in **Fig. 5** according to the spectra of the unlabeled, [$^{2}H_4$]-labeled and the [$^{13}C_{15}$]-labeled isotopologue. The concise deduction of the

structures and discussion of prior reports [27] is presented in the Electronic Supplementary Material.

Fragmentation in the electrospray ion source

The hydroxyl group of C-12a (**Fig. 3**) in the bay corner is easily eliminated during ionization, since (a) m/z 333 was detected as the precursor ion giving fragmentations (b)–(f). The intensity of (a) was almost as high as that of the precursor ion of ATX. The same occurred to the other ATXs.

To observe the loss, the temperature of ionization was reduced from 450°C to 250°C. The proportion of (a) decreased along with the intensity of target fragments. In order to insure the detection limit for ATXs as well as for other analytes, temperature was kept at 450°C. The instability of ATX indicated that for precise quantification, isotope-labeled internal standards are essential in order to compensate for the losses in MS as well as during sample preparations as far as possible.

Spectral overlap of the labeled internal standard

However, the loss of 18 Da in the ion source caused an m/z overlap between labeled und unlabeled compounds. Compared with natural substances, which have a positive increment of the molecule mass plus n (n=1, 2, 3, etc., depending on heavier natural isotopes such as ^{13}C), the [$^{13}C_{20}$]-labeled compounds have a negative increment of the molecule mass minus n originating from the ^{12}C proportion of the starting material in biosynthesis. For instance, unlabeled citric acid in the trace element solution contributed with one $^{12}C_2$ unit into the biosynthetic pathway and caused the emergence of the [$^{13}C_{18}$]isotopologue, which amounted to 40% of the

293 [$^{13}C_{20}$]isotopologue. The distribution (**Fig. 6**) was recorded in enhanced resolution mode. The
294 loss of 18 Da in the ion source yielded the same m/z as the deprotonated molecule of the
295 unlabeled analyte and a further loss of H_2O yielded fragment (a). Due to this overlap, the
296 fragments (a) in **Fig. 3** are not suitable for quantification. More details of this overlap are
297 described in the Electronic Supplementary Material.

298 <<**Fig. 6** Isotope distribution of synthesized [$^{13}C_{20}$]ATX I>>

299 Isotope distribution was measured also in the MRM mode to determine the exact purity of the
300 fully labeled internal standards and the occurrence of a spectral overlap with the unlabeled
301 analytes. The isotopic distribution of the unlabeled material confirmed the resolution of the
302 equipment, since it was in agreement with theoretical distribution of isotopologues. With these
303 results and the concentrations determined by UV spectrometry or HPLC–UV, suitable MRM
304 transitions for the five toxins were selected (**Table 3**) and MS response factors were determined,
305 which ranged from 0.98–1.11. We assume that the subtle difference of ideal response in MS is
306 caused by isotope effect (IE) due to fully labeling with ^{13}C. Moreover, the IE of AME
307 (271→256), which has been discussed above, caused the maximal deviation in response.
308 However, as the calibration curve is linear, this does not affect the accuracy of the method.

309 **Linearity**

310 Satisfying linearity of relative responses between analyte and internal standard for the chosen
311 molar ratios (0.1–10) was obtained with the coefficient of determination (R^2) exceeding 0.999 for
312 ATX I, II, alterperylenol, AOH, and AME.

Separation

The use of 2-propanol in the mobile phase not only resulted in complete separation of all analytes, but also enhanced the sensitivity. Signals were 2–7 times as intensive as those eluted with MeOH and H_2O. MeOH up to 100% was applied as the main force to elute AME to prevent an isotope effect (IE) on AME on the HPLC column in both ACN–H_2O and ACN/2-propanol–H_2O eluting system as will be detailed in the following.

Isotope effects in chromatography

When a gradient with (A) H_2O and (B) ACN/2-propanol (50/50, v/v) was used, significant and irreproducible differences in the retention time of unlabeled and ^{13}C-labeled AME were observed (**Fig. 7**), and A(An)/A(IS) ratios revealed poor reproducibility (coefficient of variation up to ±50% for AME). A possible cause for this IE was that 2-propanol possesses a higher elution strength and separation efficiency, so it could lead to a separation of multiple ^{13}C-labeled and unlabeled compounds. The differences in retention time caused a variable response in MS, probably because the different proportions of organic solvent led to different ionization efficiency, and, in consequence, in variable intensity.

<<**Fig. 7** LC-MS/MS signals of AME and [$^{13}C_{15}$]AME (dotted line) showing the isotope effect and peak tailing of [$^{13}C_{15}$]AME in the ACN/2-propanol–H_2O gradient system on Hyperclone BDS C-18 column>>

When an ACN–H_2O gradient was applied, IE on AME was not so obvious. However, no sound linear response curve was obtained as the slopes varied up to 40% if several calibration points were taken randomly. In contrast to this, IE was rarely observable for AOH, which was eluted much earlier and therefore, no separation occurred, although in principal AOH should have a similar IE behavior as AME. This indicated that elution with a more polar solvent should reduce

335 IE on ^{13}C-labeled compounds. Compared with ACN and 2-propanol, MeOH has higher polarity
336 and, therefore, did not exhibit any IE on [$^{13}C_{15}$]AME.

337 A complementary experiment with [$^{2}H_4$]AOH and [$^{2}H_4$]AME as internal standards was carried
338 out. In all systems, IE in chromatography for both substances was observed. As expected, the
339 differences in retention time of the unlabeled analytes to the deuterated standards were more
340 pronounced than to the ^{13}C-labeled standards. However, this delay remained constant, and the
341 response curve was linear with R^2 above 0.999. Unlike the ^{13}C-labeled standards, deuterium-
342 labeled standards showed a stronger but constant and predictable IE, and, therefore, the eluting
343 system is not so critical. Nevertheless, a tedious matrix calibration would be necessary for sample
344 analysis. In contrast to this, ^{13}C-labeled compounds did not show IE to that extent, except for
345 AME, which demanded a careful selection of a proper eluting system. Thus they might be better
346 choice than deuterium-labeled ones, at least in routine sample analysis.

347 Deuterated and ^{13}C-labeled compounds appear to be more polar than the unlabeled ones, since
348 both were eluted earlier than the unlabeled analytes. That the difference in properties between
349 labeled and unlabeled AME was more pronounced than that of ATXs is possibly due to the
350 planar structure of the molecule, which enables a strong interaction with the stationary phase and
351 indicates the potency of the fifteen ^{13}C atoms to convey a significant difference to the unlabeled
352 molecule.

353 **Method validation**

354 Using starch as matrix, LODs ranged from 0.09 to 0.53 µg kg^{-1}. The inter- /intra-day RSDs of the
355 method were below 13% and the recoveries ranged between 96 and 109% (**Table 4**). Compared
356 with the published validation data for ATX I including the lowest LOD at 3.0 µg kg^{-1} and a wide

357 variance in recovery [14,15], the SIDA presented here achieved a lower LOD (0.36 µg kg^{-1}), low
358 inter- /intra-day RSDs, and complete recovery even at low concentration levels. To the best of
359 our knowledge, no validation data for ATX II and alterperylenol have been published so far.

360 <<**Table 4.** Results of the method validation>>

361 As in the case of liquid samples, the MS background noise was much less; signal to noise ratios
362 of three and ten were used for estimating LODs and LOQs for these samples. Thus LODs for
363 ATX I, AOH, AME, and TEN were 0.012, 0.023, 0.010, and 0.020 µg kg^{-1}, respectively.

364 **Natural occurrence**

365 Among the measured commercial food samples (**Table 5**), organic foods tended to be more
366 frequently contaminated with ATX I and alterperylenol, as observed for some of the organic
367 whole grains (chromatograms in **Fig. 8**) and one organic apple juice.

368 <<**Fig. 8** LC–MS/MS chromatograms of an organic whole wheat flour sample>>

369 Samples with higher levels of AOH, AME, and TEN in some cases also contained ATXs, e.g.
370 paprika powder, but there were exceptions as well, since no ATXs were observed in grape juice
371 and cherry juice, although the contamination level of AOH was rather high. ATXs were not
372 detected in the analyzed tomato products. If the food was contaminated with ATXs, it was likely
373 to be co-contaminated with AOH, AME, and TEN, but not necessarily vice versa. This is in
374 agreement with the synthesis of ATXs in the later growth phase. According to their poorer
375 stability, it is predictable that ATXs contamination would be lower if the food process is more
376 elaborate. Apart from 35 food samples, 7 sorghum feed samples were analyzed and the

377 contamination level of all the analyzed toxins was more than 10 times higher than the average
378 contamination level in food samples (**Table 5**).

379 <<**Table 5.** Alternaria toxins in food samples (μg kg^{-1})>>

380 Fine and super fine wheat flour (German flour type 550 and 405, respectively) did not show any
381 contamination with the analyzed toxins. This might be a proof that *Alternaria* toxins are produced
382 strictly on the surface of grains which is exposed to oxygen and low in nutrients. ATX II, III, and
383 Ste III were not detectable. Thus they are not assumed to be a health hazard in the food chain
384 because they are not stable. However, special attention should be paid to *Alternaria* spores and
385 they should be avoided because they might contain those mutagenic toxins.

386 For a solid risk assessment of ATXs for consumers, neither enough toxicological nor accurate
387 exposure data are available. However, with the data presented here, a first estimation for ATX I
388 can be done on the basis of the threshold of toxicological concern (TTC) approach generally
389 applied by the EFSA in such cases with the following assumptions: (1) As a genotoxic
390 compound, ATX I can be classified in the group of compounds containing alerts of
391 carcinogenicity resulting in a TTC threshold of 0.15 μg day^{-1} [28], (2) as we detected ATX I
392 mainly in organic whole cereals or the respective flours, only these kinds of products were
393 considered to be a potential risk for the respective consumers and to contain a calculative mean of
394 1.23 μg kg^{-1} ATX I, and (3) we considered the average daily consumption of cereals and cereals
395 products of 70 and 58 g per day for men and women, respectively, as an conservative estimate
396 [29]. Under these assumptions, the mean chronic dietary exposure to ATX I for consumers of
397 whole cereals and cereal products is estimated to be 0.086 and 0.071 μg per day for men and
398 women, respectively, which does not exceed the TTC value of 0.15 μg day^{-1}.

Conclusions

The study on labeled ATXs has indicated that directed biosynthesis in chemically defined media can achieve selective production of mycotoxins. This can not only increase the yield but also reduces by-products and thus facilitates purification. To obtain higher amounts of stable isotope-labeled internal standards for highly accurate analysis, there is much more work necessary to explore biosynthesis, especially when chemical synthesis is not feasible.

The results of the first comprehensive SIDA presented here indicate that the main exposure to ATX originates from cereals and that bread does not contribute to ATX exposure. This finding can be attributed to the instability of ATX toxins to heat treatment. Thus our present data point to an exposure below the TTC, and, therefore, we do not conclude an urgent need for measures of reduction. However, the TTC concept includes several imponderables such as the threshold set ambiguously and the highly variable consumption data. Moreover, as our data on cereals and bread are far from being representative, we recommend further monitoring of ATX contamination in foods. In addition, a reliable risk assessment requires additional compound-specific toxicity data.

In addition, in feed the higher amounts of ATXs might be critical.

Acknowledgments

We gratefully acknowledge Dr. Oliver Frank, Chair of Food Chemistry and Molecular Sensory Science, TU München, for the NMR measurements. We thank Andrea Backhaus, Chair of Phytopathology, TU München, for providing us the *Alternaria* strains. Moreover, we thank the Faculty Graduate Center Weihenstephan of TUM Graduate School and the program ‘Equal

opportunity for women in research and teaching' of TU München for providing a scholarship for YL.

Appendix A. Electronic Supplementary Material

References

1. Chu FS (1981) Isolation of altenuisol and altertoxins I and II, minor mycotoxins elaborated by alternaria. J Am Oil Chem Soc 58 (12):1006–1008

2. Pero RW, Posner H, Blois M, Harvan D, Spalding JW (1973) Toxicity of metabolites produced by the "Alternaria". Environ Health Perspect 4:87–94

3. Robeson D, Strobel G, Matusumoto GK, Fisher EL, Chen MH, Clardy J (1984) Alteichin: an unusual phytotoxin fromAlternaria eichorniae, a fungal pathogen of water hyacinth. Experientia 40 (11):1248–1250

4. Arnone A, Nasini G, Merlini L, Assante G (1986) Secondary mould metabolites. Part 16. Stemphyltoxins, new reduced perylenequinone metabolites from Stemphylium botryosum var. Lactucum. J Chem Soc, Perkin Trans 1 (0):525–530

5. Okuno T, Natsume I, Sawai K, Sawamura K, Furusaki A, Matsumoto T (1983) Structure of antifungal and phytotoxic pigments produced by alternaria sps. Tetrahedron Lett 24 (50):5653–5656

6. Stack ME, Prival MJ (1986) Mutagenicity of the Alternaria metabolites altertoxins I, II, and III. Appl Environ Microbiol 52 (4):718–722

7. Fleck SC, Burkhardt B, Pfeiffer E, Metzler M (2012) Alternaria toxins: Altertoxin II is a much stronger mutagen and DNA strand breaking mycotoxin than alternariol and its methyl ether in cultured mammalian cells. Toxicol Lett 214 (1):27–32

8. Davis VM, Stack ME (1991) Mutagenicity of stemphyltoxin III, a metabolite of Alternaria alternata. Appl Environ Microbiol 57 (1):180–182

9. EFSA. (2011) EFSA Panel on Contaminants in the Food Chain. Scientific Opinion on the risks for animal and public health related to the presence of Alternaria toxins in feed and food. EFSA J 9:2407−2504

10. Wittkowski M, Baltes W, Krönert W, Weber R (1983) Bestimmung von Alternaria-Toxinen in Obst- und Gemüseerzeugnissen. Zeitschrift für Lebensmittel-Untersuchung und Forschung 177 (6):447–453

448 11. Visconti A, Sibilia A, Palmisano F (1991) Selective determination of altertoxins by high-performance
449 liquid chromatography with electrochemical detection with dual “in-series” electrodes. J Chromatogr, A
450 540 (0):376–382
451 12. Adb El-Aal SS (1997) Effects of gamma radiation, temperature and water activity on the production of
452 Alternaria mycotoxins. Egypt J Microbiol 32:379–396
453 13. Scott PM (2001) Analysis of agricultural commodities and foods for Alternaria mycotoxins. J AOAC
454 Int 84:1809–1817
455 14. Warth B, Parich A, Atehnkeng J, Bandyopadhyay R, Schuhmacher R, Sulyok M, Krska R (2012)
456 Quantitation of mycotoxins in food and feed from Burkina Faso and Mozambique using a modern LC-
457 MS/MS multitoxin method. J Agric Food Chem 60 (36):9352–9363
458 15. Varga E, Glauner T, Berthiller F, Krska R, Schuhmacher R, Sulyok M (2013) Development and
459 validation of a (semi-)quantitative UHPLC-MS/MS method for the determination of 191 mycotoxins and
460 other fungal metabolites in almonds, hazelnuts, peanuts and pistachios. Anal Bioanal Chem 405
461 (15):5087–5104
462 16. Streit E, Schwab C, Sulyok M, Naehrer K, Krska R, Schatzmayr G (2013) Multi-mycotoxin screening
463 reveals the occurrence of 139 different secondary metabolites in feed and feed ingredients. Toxins (Basel)
464 5:504–523
465 17. Jensen B, Knudsen IMB, Andersen B, Nielsen KF, Thrane U, Jensen DF, Larsen J (2013)
466 Characterization of microbial communities and fungal metabolites on field grown strawberries from
467 organic and conventional production. Int J Food Microbiol 160 (3):313–322
468 18. Pozzi CR, Braghini R, Arcaro JRP, Zorzete P, Israel ALM, Pozar IO, Denucci S, Correa B (2005)
469 Mycoflora and occurrence of alternariol and alternariol monomethyl ether in Brazilian sunflower from
470 sowing to harvest. J Agric Food Chem 53:5824–5828
471 19. Asam S, Konitzer K, Schieberle P, Rychlik M (2009) Stable isotope dilution assays of alternariol and
472 alternariol monomethyl ether in beverages. J Agric Food Chem 57:5152–5160
473 20. Liu Y, Rychlik M (2013) Development of a stable isotope dilution LC−MS/MS method for the
474 Alternaria toxins tentoxin, dihydrotentoxin, and isotentoxin. J Agric Food Chem 61 (12):2970–2978
475 21. Hradil CM, Hallock YF, Clardy J, Kenfield DS, Strobel G (1989) Phytotoxins from Alternaria cassiae.
476 Phytochem 28 (1):73–75
477 22. Stack ME, Mazzola EP, Page SW, Pohland AE, Highet RJ, Tempesta MS, Corley DG (1986)
478 Mutagenic Perylenequinone Metabolites of Alternaria alternata: Altertoxins I, II, and III. J Nat Prod 49
479 (5):866–871

480 23. Schwarz C, Tiessen C, Kreutzer M, Stark T, Hofmann T, Marko D (2012) Characterization of a
481 genotoxic impact compound in Alternaria alternata infested rice as Altertoxin II. Arch Toxicol 86
482 (12):1911–1925
483 24. Leslie JF, Summerell BA, Bullock S (2006) The Fusarium Laboratory Manual. Wiley-Blackwell,
484 Chichester, U.K.
485 25. Korn M, Frank O, Hofmann T, Rychlik M (2011) Development of stable isotope dilution assays for
486 ochratoxin A in blood samples. Anal Biochem 419:88–94
487 26. Vogelgesang J, Haedrich J (1998) Limits of detection, identification and determination: a statistical
488 approach for practitioners. Accredit Qual Assur 3:242–255
489 27. Lau BPY, Scott PM, Lewis DA, Kanhere SR, Cléroux C, Roscoe VA (2003) Liquid chromatography–
490 mass spectrometry and liquid chromatography–tandem mass spectrometry of the Alternaria mycotoxins
491 alternariol and alternariol monomethyl ether in fruit juices and beverages. J Chromatogr A 998 (1–2):119–
492 131
493 28. Kroes R, Renwick AG, Cheeseman M, Kleiner J, Mangelsdorf I, Piersma A, Schilter B, Schlatter J,
494 van Schothorst F, Vos JG, Würtzen G (2004) Structure-based thresholds of toxicological concern (TTC):
495 guidance for application to substances present at low levels in the diet. Food Chem Toxicol 42:65–83
496 29. DGE. (2012) 12. Ernährungsbericht. Deutsche Gesellschaft für Ernährung e. V., Bonn, Germany

497

Tables

Table 1. Characterization of ATXs

	Precursor ion (m/z, negative)	**Fragment ions** (*m/z*, negative)	**UV** (MeOH) λ_{max} in nm (logε in L/mol/cm)	**^{1}H NMR** (500 MHz, D_4-MeOH) δ (ppm)
ATX I	351	333, 315, 314, 305, 297, 263	215(4.54) 257(4.66) 284(4.35) 352(3.86)	2.37–2.47 (m, 1 H), 2.64–2.68 (m, 1 H), 2.94 (d, *J*=11.30 Hz, 1 H), 2.99 (d, *J*=5.02 Hz, 1 H), 3.04–3.06 (m, 1 H), 3.07–3.16 (m, 1 H), 3.12 (s, 1 H), 4.62–4.67 (m, 1 H), 6.97 (d, *J*=8.79 Hz, 1 H), 7.06 (d, *J*=8.79 Hz, 1 H), 7.96 (d, *J*=8.79 Hz, 1 H), 8.01 (d, *J*=9.10 Hz, 1 H).
Alterperylenol	349	331, 313, 303, 261	215(4.61) 255(4.64) 285(4.41) 364(3.82)	2.86–2.93 (m, 1 H), 3.04 (d, *J*=10.99 Hz, 1 H), 3.16 (s, 1 H), 4.59–4.65 (m, 1 H), 6.34 (d, *J*=10.36 Hz, 1 H), 6.98 (d, *J*=9.73 Hz, 1 H), 7.06 (d, *J*=8.79 Hz, 1 H), 7.91 (d, *J*=10.36 Hz, 1 H), 7.96 (d, *J*=8.79 Hz, 1 H), 8.02 (d, *J*=8.79 Hz, 1 H).
ATX II	349	331, 329, 313, 303, 301, 285	215(4.49) 259 (4.54) 361(3.90)	2.49 (td, *J*=13.81, 4.08 Hz, 1 H), 2.79 (m, 1 H), 2.88 (m, 1 H), 3.16–3.27 (m, 1 H), 3.58 (s, 1 H), 3.69 (d, *J*=4.08 Hz, 1 H), 4.35 (d, *J*=3.45 Hz, 1 H), 7.01 (d, *J*=8.79 Hz, 1 H), 7.09 (d, *J*=8.79 Hz, 1 H), 8.01 (d, *J*=8.79 Hz, 1 H), 8.10 (d, *J*=9.10 Hz, 1 H).

Ste III	347	330, 329, 301, 285	217(4.38) 271(4.42) 374(3.71)	3.72 (d, *J*=3.77 Hz, 1 H), 3.80 (s, 1 H), 4.47 (d, *J*=3.77 Hz, 1 H), 6.55 (d, *J*=10.36 Hz, 1 H), 7.02 (d, *J*=8.79 Hz, 1 H), 7.09 (d, *J*=9.10 Hz, 1 H), 7.70 (d, *J*=10.36 Hz, 1 H), 8.06 (d, *J*=5.65 Hz, 1 H), 8.07 (d, *J*=5.65 Hz, 1 H).
ATX III	347	319, 277	267, 350	

501

502

503 **Table 2.** MS fragmentation of ^{13}C-labeled toxins in negative ESI mode

	Precursor ion (m/z)	**Fragment ions** (*m/z*)
[$^{13}C_{20}$]ATX I	371	353, 335, 334, 317, 280
[$^{13}C_{20}$]Alterperylenol	369	351, 333, 322, 278
[$^{13}C_{20}$]ATX II	369	351, 333, 322, 304
[$^{13}C_{20}$]Ste III	367	350, 349, 320, 304
[$^{13}C_{20}$]ATX III	367	338, 294
[$^{13}C_{14}$]AOH	271	227, 226, 225, 169, 168, 156
[$^{13}C_{15}$]AME	286	270, 269, 241, 240, 225, 195
[$^{13}C_{15}$]ALT	306	288, 261, 243, 227
[$^{13}C_{14}$]AS	287	271, 197, 196, 184

504

505

506 **Table 3.** Compound-dependent parameters in MRM (negative) mode on LC–MS/MS.

Compound	**RT** (min)	**MRM** (*m/z*)	**DP** (V)	**CE** (V)	**A(a)/ A(b)** [d]	**Compound**	**RT** (min)	**MRM** (*m/z*)	**DP** (V)	**CE** (V)	**A(a)/ A(b)** [d]
ALT	7.38	291→229 [a]	–54	–25	2.0	**AS**	13.11	273→258 [a]	–65	–32	4.8
		291→247 [b]	–54	–25				273→186 [b]	–65	–48	
[$^{13}C_{15}$]ALT	7.35	306→243 [a]	–54	–25	2.0	**[$^{13}C_{14}$]AS**	13.09	287→271 [a]	–65	–32	4.8
		306→261 [b]	–54	–25				287→197 [b]	–65	–48	
ATX I	9.98	351→314 [a]	–54	–40	0.2	**TEN** [c]	13.53	413→141 [a]	–80	–30	1.5
		351→297 [a]	–54	–36	0.2			413→271 [b]	–80	–25	
		351→315 [b]	–54	–22		**[$^{2}H_3$]TEN** [c]	13.50	416→141 [a]	–80	–30	1.5
[$^{13}C_{20}$]ATX I	9.95	371→334 [a]	–54	–40	0.2			416→274 [b]	–80	–25	
		371→317 [a]	–54	–36	0.2	**ATX II**	14.62	349→313 [a]	–54	–32	0.2
		371→335 [b]	–54	–22				349→331 [b]	–54	–20	
Alterperylenol	10.77	349→261 [a]	–54	–36	1.4	**[$^{13}C_{20}$]ATX II**	14.56	369→333 [a]	–54	–32	0.2
		349→303 [b]	–54	–34				369→351 [b]	–54	–20	
[$^{13}C_{20}$]Alterperylenol	10.75	369→278 [a]	–54	–36	1.4	**AME**	19.75	271→256 [a]	–65	–30	6.2
		369→322 [b]	–54	–34				271→228 [b]	–65	–44	
AOH	12.03	257→147 [a]	–65	–46	0.5	**[$^{13}C_{15}$]AME**	19.72	286→270 [a]	–65	–30	6.2
		257→213 [b]	–65	–32				286→241 [b]	–65	–44	
[$^{13}C_{14}$]AOH	12.01	271→156 [a]	–65	–46	0.5						
		271→226 [b]	–65	–32							

507 [a] MRM used as quantifier, depending on matrix if two quantifiers are given, [b] MRM used as qualifier, [c] published
508 parameters of TEN and [$^{2}H_3$]TEN [20], [d] quantifier/qualifier ion ratio, CE: collision energy, DP: declustering
509 potential, RT: retention time.

510

511 **Table 4.** Results of the method validation

Analyte	LOD	LOQ	Precision (RSD, %)		Recovery (%)	
	(µg/kg)	(µg/kg)	Intra-day (n=6)	Inter-day (n=3)	Spike: 1.6 µg/kg	Spike: 4 µg/kg
ATX I	0.36	1.1	6.1	8.7	102 ± 8	105 ± 3
Alterperylenol	0.20	0.58	5.7	3.8	98 ± 3	96 ± 4
ATX II	0.53	1.6	9.1	9.9	(-)	101 ± 9
AOH	0.36	1.1	13	4.1	103 ± 4	98 ± 4
AME	0.088	0.27	3.3	5.8	112 ± 7	109 ± 3

512 * LOD, LOQ, and recovery were determined in potato starch as the matrix; (-), data not available.

513

514

515 **Table 5.** Alternaria toxins in food samples (μg kg^{-1})

Sample name [a)]	ATX I	Alterperylenol	ATX II	AOH	AME	TEN [c)]
organic whole wheat flour	4.0	n.q.	-	23	n.q.	-
organic wheat flour	-	-	-	-	-	n.q.
whole wheat flour	-	-	-	-	-	2.9
fine and super fine wheat flour (2)	-	-	-	-	-	-
organic whole spelt flour (2)	n.d.–2.4	n.d.–n.q.	-	1.4–12	0.31–0.34	n.q.–1.6
	1.3 [b)]	0.25 [b)]	-	6.6 [b)]	0.32 [b)]	0.96 [b)]
whole spelt flour	-	-	-	-	-	-
organic whole rye flour (2)	n.d.–4.7	n.d.–0.87	-	n.d.–1.1	n.d.–0.32	3.9–6.0
	2.4 [b)]	0.49 [b)]	-	0.66 [b)]	0.18 [b)]	4.9 [b)]
oats	-	-	-	-	-	-
millet	-	-	-	-	-	-
organic pumpernickel bread	-	-	-	-	-	5.5
organic whole rye sourdough bread with sunflower seeds	-	2.7	-	-	-	3.7
mixed sourdough bread	-	-	-	-	-	0.94
whole rye crispbread	-	5.4	-	-	-	5.4
paprika powder (3)	n.d.–4.2	n.d.–5.2	-	17–46	14–26	26–80
	2.5 [b)]	2.9 [b)]	-	31 [b)]	21 [b)]	47 [b)]
spice mix	-	-	-	12	4.3	2.7
parsley	-	-	-	-	-	-
sunflower seed (raw, without hull)	-	-	-	-	-	8.3
roasted sunflower seed (with hull)	-	-	-	1.9	9.0	-
tomato ketchup (2)	-	-	-	(-)	(-)	-
tomato paste	-	-	-	(-)	(-)	3.2

apple juice (5)	-	-	-	-	-	-
organic apple juice	0.040	-	-	(-)	(-)	(-)
grape juice	-	-	-	7.1	0.061	0.065
tomato juice	-	-	-	0.076	n.q.	0.089
cherry juice	-	-	-	4.0	0.34	0.18
sorghum feed (7)	37–52	38–74	n.d.–1.7	347–757	109–215	33–75
	43 [b)]	58 [b)]	1.0 [b)]	521 [b)]	164 [b)]	55 [b)]

-, not detected; n.q., not quantifiable; (-), not analyzed;

[a)] number of samples other than one in parentheses,

[b)] mean values, (LOQ + LOD)/2 was used for not quantifiable values and LOD/2 for not detectable values,

[c)] referring to LOD (0.18 µg kg^{-1}) and LOQ (0.54 µg kg^{-1}) for TEN [20].

Captions to the Figures

Fig. 1 Structures of ATXs

Fig. 2 Structures of AOH, AME, and TEN

Fig. 3 Proposed fragmentation of ATXs. (A) ATX I, (B) Alterperylenol, (C) ATX II, (D) ATX III, (E) Ste III. In parentheses: the respective m/z data of the completely ^{13}C-labeled isotopologue.

Fig. 4 MS spectra of labeled and unlabeled AOH and proposed fragmentation to the quantifier. In parentheses: the respective *m/z* data of the completely ^{13}C-labeled isotopologue. In square brackets: the respective *m/z* data of the isotopologue with four ^{2}H-labelings in the aromatic rings.

Fig. 5 MS spectra of labeled and unlabeled AME and proposed fragmentation. In parentheses: the respective m/z data of the completely ^{13}C-labeled isotopologue. In square brackets: the respective m/z data of the isotopologue with four ^{2}H-labelings in the aromatic rings.

Fig. 6 Isotope distribution of synthesized [$^{13}C_{20}$]ATX I

Fig. 7 LC-MS/MS signals of AME and [$^{13}C_{15}$]AME (dotted line) showing the isotope effect and peak tailing of [$^{13}C_{15}$]AME in the ACN/2-propanol–H_2O gradient system on Hyperclone BDS C-18 column

Fig. 8 LC–MS/MS chromatograms of an organic whole wheat flour sample

Figures

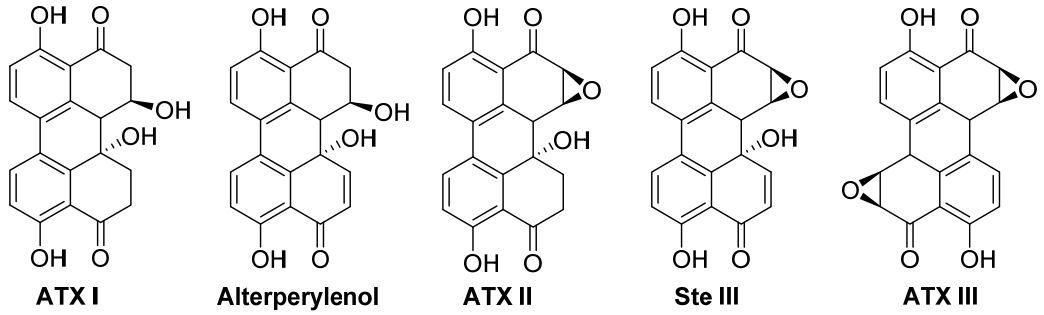

Fig. 1 Structures of ATXs

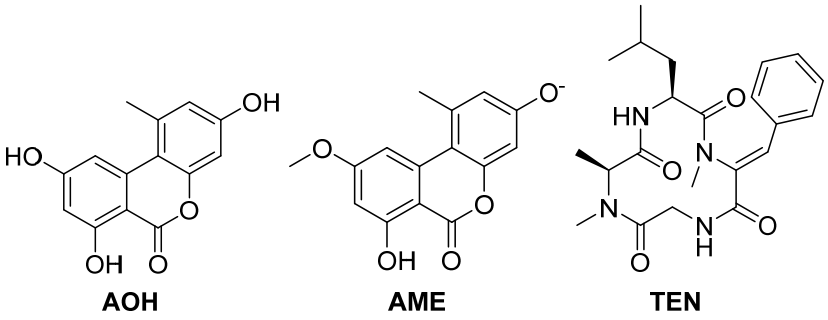

Fig. 2 Structures of AOH, AME, and TEN

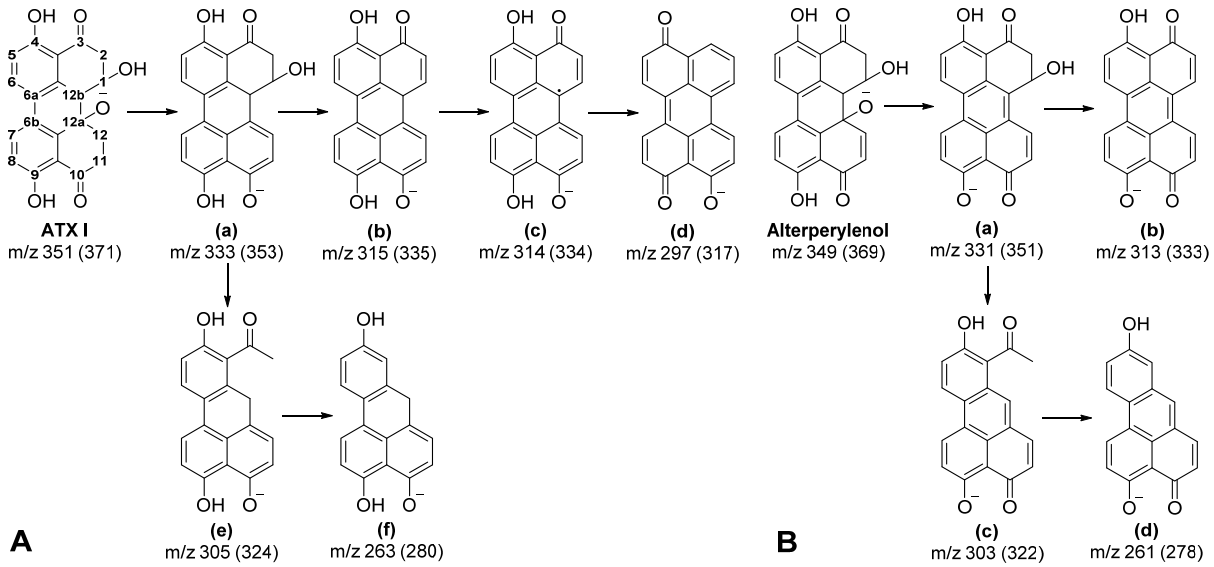
ATX I
m/z 351 (371)
(a)
m/z 333 (353)
(b)
m/z 315 (335)
(c)
m/z 314 (334)
(d)
m/z 297 (317)
(e)
m/z 305 (324)
(f)
m/z 263 (280)
A
Alterperylenol
m/z 349 (369)
(a)
m/z 331 (351)
(b)
m/z 313 (333)
(c)
m/z 303 (322)
(d)
m/z 261 (278)
B

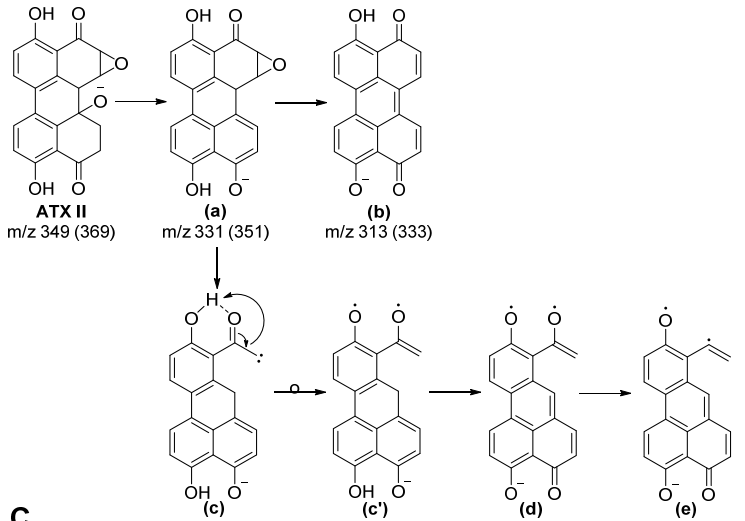
ATX II
m/z 349 (369)
(a)
m/z 331 (351)
(b)
m/z 313 (333)
(c)
m/z 303 (322)
(c')
m/z 303 (322)
(d)
m/z 301 (320)
(e)
m/z 285 (304)
C

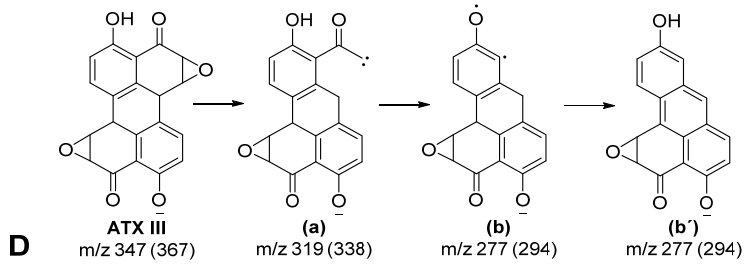
ATX III
m/z 347 (367)
(a)
m/z 319 (338)
(b)
m/z 277 (294)
(b´)
m/z 277 (294)
D

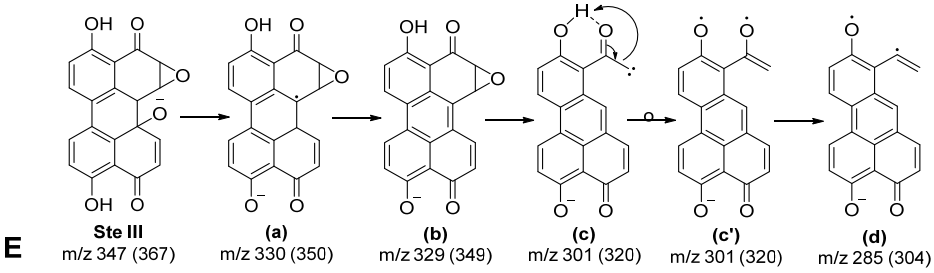

Fig. 3 Proposed fragmentation of ATXs. (**A**) ATX I. (**B**) Alterperylenol. (**C**) ATX II. (**D**) ATX III. (**E**) Ste III. In parentheses: the respective m/z data of the completely ^{13}C-labeled isotopologue.

560

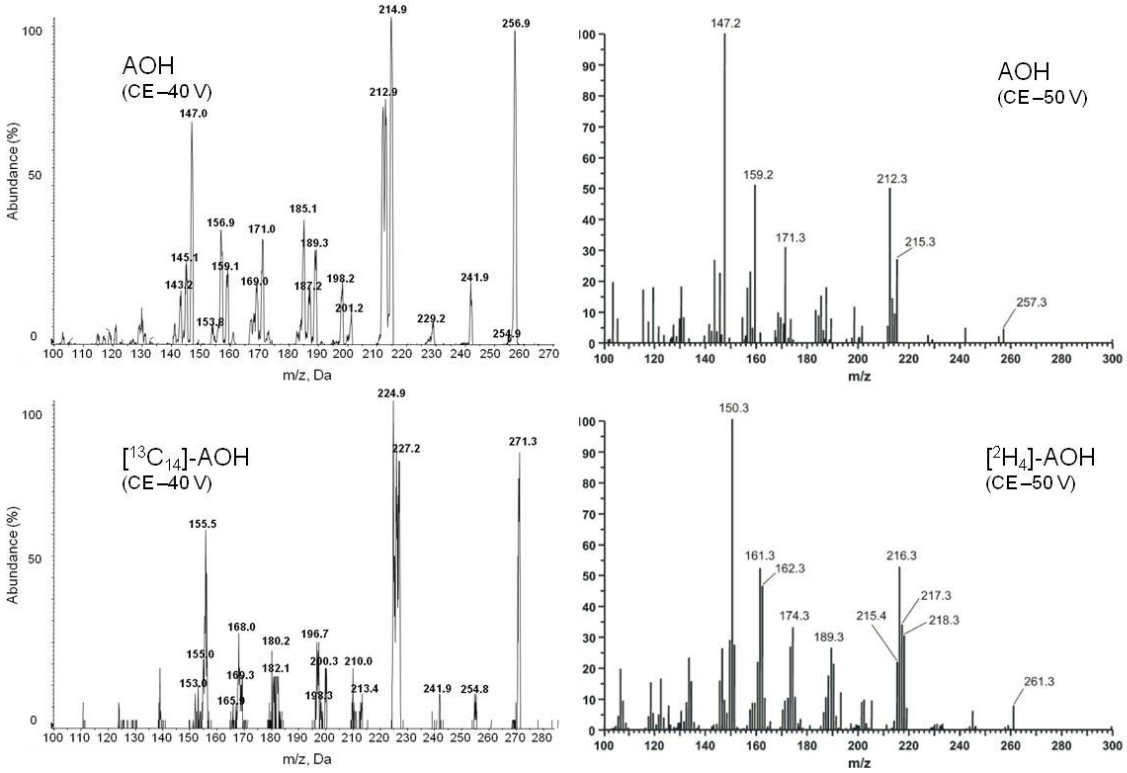

561

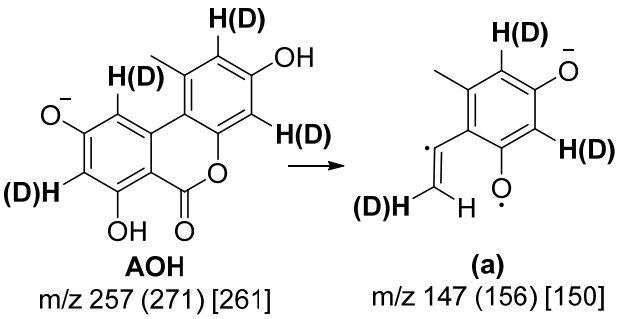

562 **Fig. 4 MS spectra of labeled and unlabeled AOH and proposed fragmentation to the quantifier.** In parentheses:
563 the respective *m/z* data of the completely ^{13}C-labeled isotopologue. In square brackets: the respective *m/z* data of the
564 isotopologue with four ^{2}H-labelings in the aromatic rings.

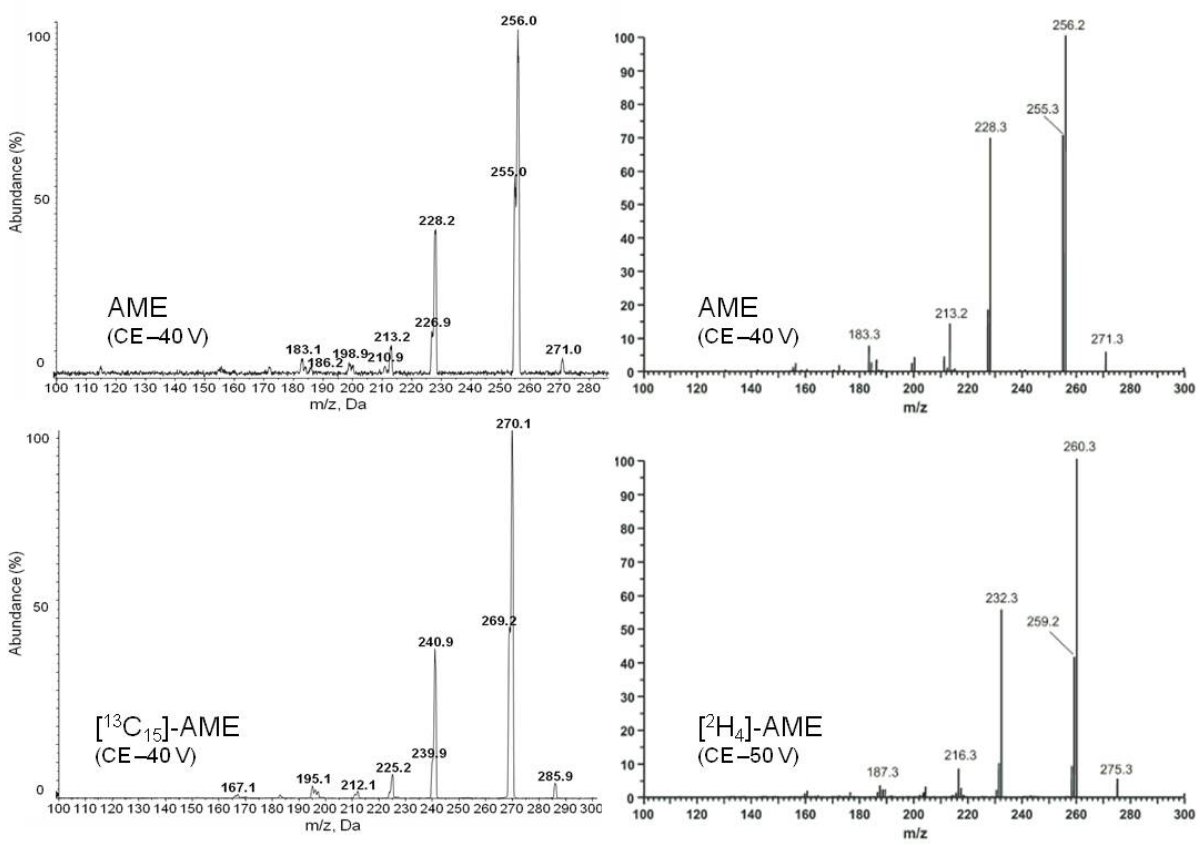
AME
(CE –40 V)
256.0
255.0
228.2
226.9
213.2
183.1
186.2
198.9
210.9
271.0
Abundance (%)
m/z, Da
AME
(CE –40 V)
256.2
255.3
228.3
213.2
183.3
271.3
m/z
[13C15]-AME
(CE –40 V)
270.1
269.2
240.9
239.9
225.2
195.1
212.1
167.1
285.9
Abundance (%)
m/z, Da
[2H4]-AME
(CE –50 V)
260.3
232.3
259.2
216.3
187.3
275.3
m/z

565

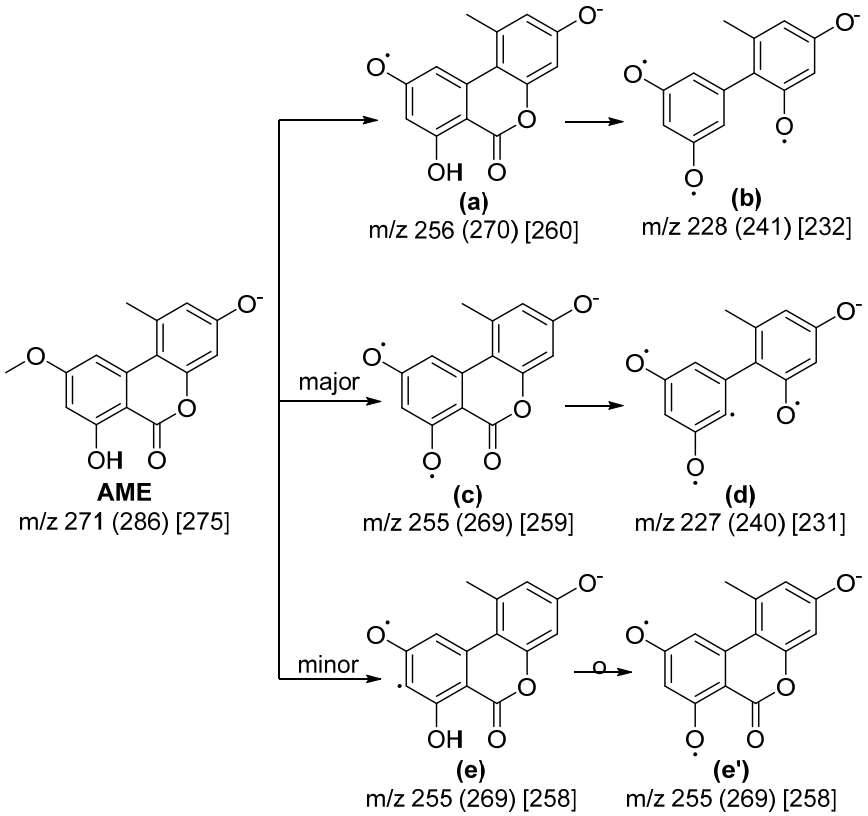

566

567 **Fig. 5 MS spectra of labeled and unlabeled AME and proposed fragmentation.** In parentheses: the respective

568 m/z data of the completely ^{13}C-labeled isotopologue. In square brackets: the respective m/z data of the isotopologue

569 with four ^{2}H-labelings in the aromatic rings.

570

571

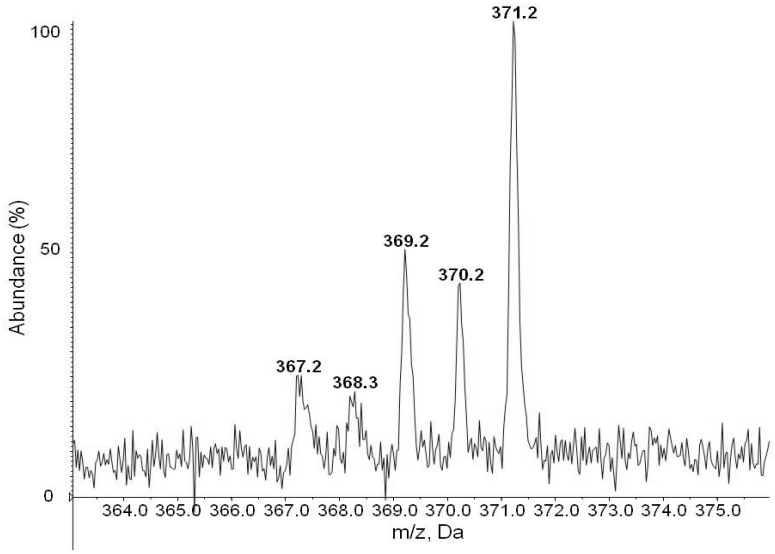

572 **Fig. 6** Isotope distribution of synthesized [$^{13}C_{20}$]ATX I

573

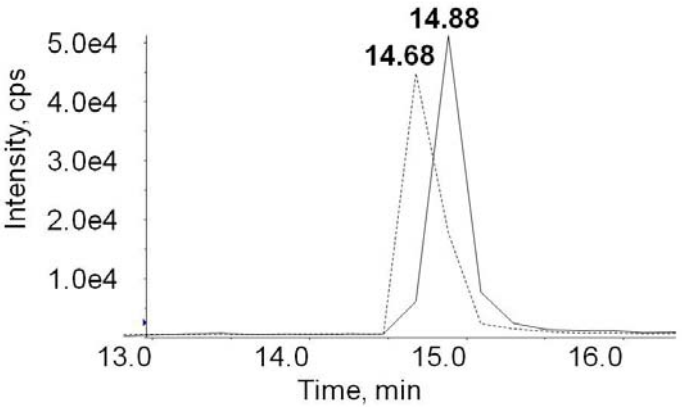

574

575 **Fig. 7** LC-MS/MS signals of AME and [$^{13}C_{15}$]AME (dotted line) showing the isotope effect and peak tailing of

576 [$^{13}C_{15}$]AME in the ACN/2-propanol–H_2O gradient system on Hyperclone BDS C-18 column

577

578 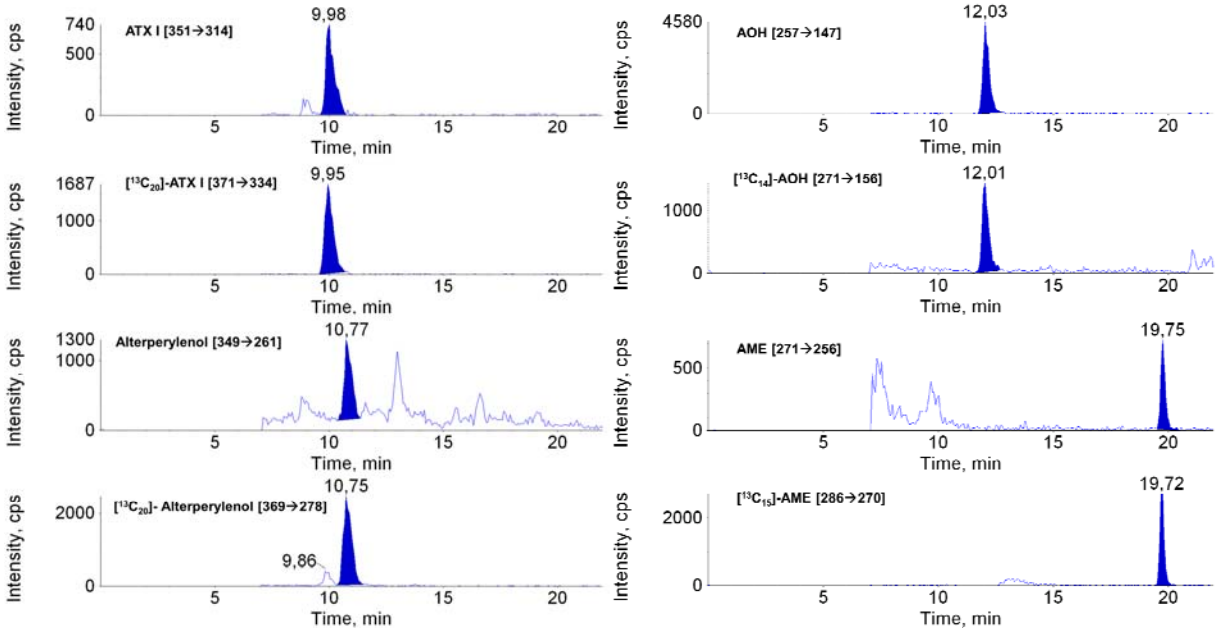

579 **Fig. 8** LC–MS/MS chromatograms of an organic whole wheat flour sample

580